



## University of Dundee

An integrated CRITIC-COPRAS approach for multi-response optimization on AWJM of hybrid filler–reinforced polymer composite and its surface integrity

Vijayananth, Kavimani; Muthukutti, Gopal Pudhupalayam; Ramakrishnan, Sumesh Keerthiveetil; Venkatesan, Sivamaran; Zhou, Wenbin

DOI:

[10.1007/s00170-024-13267-7](https://doi.org/10.1007/s00170-024-13267-7)

Publication date:

2024

Licence:

CC BY

Document Version

Publisher's PDF, also known as Version of record

[Link to publication in Discovery Research Portal](#)

*Citation for published version (APA):*

Vijayananth, K., Muthukutti, G. P., Ramakrishnan, S. K., Venkatesan, S., & Zhou, W. (2024). An integrated CRITIC-COPRAS approach for multi-response optimization on AWJM of hybrid filler–reinforced polymer composite and its surface integrity. *The International Journal of Advanced Manufacturing Technology*, 131(9-10), 4965-4980. <https://doi.org/10.1007/s00170-024-13267-7>

### General rights

Copyright and moral rights for the publications made accessible in Discovery Research Portal are retained by the authors and/or other copyright owners and it is a condition of accessing publications that users recognise and abide by the legal requirements associated with these rights.

### Take down policy

If you believe that this document breaches copyright please contact us providing details, and we will remove access to the work immediately and investigate your claim.



# An integrated CRITIC-COPRAS approach for multi-response optimization on AWJM of hybrid filler–reinforced polymer composite and its surface integrity

Kavimani Vijayananth<sup>1,2</sup> · Gopal Pudhupalayam Muthukutti<sup>1,2</sup> · Sumesh Keerthiveetil Ramakrishnan<sup>3</sup> · Sivamaran Venkatesan<sup>4</sup> · Wenbin Zhou<sup>5,6</sup> 

Received: 28 October 2023 / Accepted: 14 February 2024 / Published online: 29 February 2024

© The Author(s) 2024

## Abstract

Composites have gained acceptance in an extensive range of applications owing to their unique characteristics. But, machining of these materials is often challenging due to improved bonding between matrix and fibre when fillers are added. Since the machinability is an important aspect for any material for its successful utilization, it is essential to analyse the effect of secondary phase on machinability. However, investigations on the effect of fillers on machinability of polymer composites are minimal. In this research, hybrid fillers, namely boron nitride (BN) and montmorillonite (MMT) nanoclay, were added to epoxy/glass fibre composite through compression moulding, in which quantity of MMT is fixed and BN is varied from 2 to 6 wt%. Abrasive water jet machining (AWJM) is a leading method for machining polymer composites in which transverse speed, stand-off distance, pump pressure and filler percentage are key factors and are considered as input variables. To assess the machinability, material removal rate (MRR), surface roughness (Ra) and kerf taper (Kt) are chosen as response variables. Experimental planning is done through Taguchi method, and Criteria Importance Through Intercriteria Correlation (CRITIC)-weighted Complex Proportional Assessment (COPRAS) technique is utilized for optimization. The results revealed that addition of BN reduces the MRR while it improves the surface finish and reduces the Kt. Transverse speed has the most influence over all the considered output responses, stand-off distance and water pressure mainly affect the MRR and Ra while filler addition mainly affects the Kt. The hybrid CRITIC-COPRAS approach–recommended optimal control factors resulted in 16.20 mm<sup>3</sup>/min MRR with 0.29° Kt and 3.86 µm Ra. The recommended optical condition can be utilized for effective machining of polymer composite with MMT/BN fillers.

**Keywords** Nano filler · Composite · Water jet machining · Optimization · Surface integrity

✉ Kavimani Vijayananth  
manikavi03@gmail.com

✉ Wenbin Zhou  
wzhou001@dundee.ac.uk

Gopal Pudhupalayam Muthukutti  
gopal33mech@gmail.com

Sumesh Keerthiveetil Ramakrishnan  
sumesh2311@gmail.com

Sivamaran Venkatesan  
Sivamaran.venkatesan@ul.ie

<sup>1</sup> Centre for Material Science, Karpagam Academy of Higher Education, Coimbatore 641 021, India

<sup>2</sup> Department of Mechanical Engineering, Karpagam Academy of Higher Education, Coimbatore 641 021, India

<sup>3</sup> Department of Materials Engineering, Faculty of Mechanical Engineering, Czech Technical University in Prague, Prague, Czech Republic

<sup>4</sup> The Pharmaceutical Manufacturing Technology Centre (PMTTC), Bernal Institute, University of Limerick, Limerick, Ireland

<sup>5</sup> School of Science and Engineering, University of Dundee, Dundee DD1 4HN, UK

<sup>6</sup> Department of Mechanical Engineering, Imperial College London, London SW7 2AZ, UK

## 1 Introduction

Owing to their unique qualities, viz. light weight, high strength-to-weight ratio, high modulus and rigidity with excellent chemical stability [1–3], fibre-reinforced polymer (FRP) composites are now being utilized in various industrial applications including marine, spacecraft, transportation and building industries. Nowadays, research has been conducted on FRP composites that have been changed with filler additions. It has been discovered that adding filler materials over base polymer matrix improves their dimensional stability and modulus [4, 5]. Minerals, carbon and nitride-based materials such as montmorillonite, carbon nanotube, graphene and boron nitride improve the flame retardancy and mechanical behaviour of base matrix while used as filler materials in FRP. These filler materials initiate stress transfer from the matrix to fibre. Addition of fillers in FRP showcases more effectiveness in increasing stiffness, strength and fracture toughness [6–8]. On the other hand, improved bonding of fibre and matrix with the presence of fillers leads to poor machinability.

Even after developing near-net form FRP composites, machining activities are the other parts of finishing process that are still necessary and are controlled by a few key requirements, such as fulfilling the complex shape and precise dimensional and functional specifications. Prior to assembly, the key activity in the production process that gives the FRP composites their final, intended shape frequently involves machining [9, 10]. Traditional processing methods such as band saw cutting result in not only low-cut quality but also low productivity, while the non-traditional laser cutting technology has been found to yield large burr formation, dimensional inaccuracy due to thermal distortion, heat-affected zone (or burnt) and even fire hazard for these heat-sensitive materials [11, 12]. The unique ‘cold’ abrasive water jet (AWJ) cutting technology, due to its distinct advantages of no thermal distortion, high machining versatility, high flexibility and small cutting forces, offers great potential for the processing of polymer matrix composites. During abrasive water jet machining (AWJM) process, water jet removes eroded material from workpiece and decreases possibility of environmental pollution caused by fibrous materials [13, 14]. The formation of kerf taper, delamination, surface roughness, abrasive embedment, fibre pull-out and other limitations related to AWJ cutting reduce the quality of the fabricated components [15, 16]. Proper selection and optimization of machining control factors will definitely make the AWJM process more efficient.

Occurrence of delamination, taper in the cut edges and rough surface finishes during AWJM weakens the composite structures and affects dimensional accuracy that

requires post-machining finishing operations for achieving the desired surface quality. Hence, there is a need to improve the machinability of polymer composite. Optimization of machining parameter is one of the ways to improve the machining performance of polymer composite [17, 18]. Parameter optimization in AWJM plays a pivotal role in achieving high-quality cuts, efficient material removal and overall process optimization. There are few reported studies related to machining and optimization of AWJM of FRP composite. Chenrayan et al. [19] adopted hybrid grey relational-based principal component analysis to attain optimal parameter for achieving minimal kerf width and delamination damages. The control factors such as stand-off distance (SOD), abrasive mass flow rate (MF), water pressure (WP) and transverse speed (TS) are selected. Results depicted that WP and MF act as key parameters for influencing kerf width, and that minimal levels of SOD and MR decrease the delamination damages in developed composite. Iyer and Arunkumar [20] developed FRP composite and investigated the AWJM parameters by using response surface analysis. Herein, water pressure, TS, SOD and MF are selected as machining parameters and surface roughness and kerf taper are as output responses [20]. Results showed that TS has foremost influence on output response, an increase in MF and TS leads to fibre delamination while minimal values of TS, water pressure and MF increase the quality of machined surface. Juvvala et al. [21] fabricated nano montmorillonite (MMT) filler-reinforced FRP composite and adopted AWJM process to investigate the machinability of the developed FRP. Herein, varying percentages of MMT, TS, MF and SOD are selected as machining parameters and delamination factor as an output response [21]. Results revealed that an increase in MMT addition decreases the delamination factor, and it was suggested that moderate MF and SOD minimize the delamination. Thakur and Singh [22] utilized graphene as the filler material to develop FRP composite and investigated the machinability behaviour using AWJM. Wt% of filler, transverse rate and jet pressure are used as machining factors, and surface roughness and kerf angle are selected as output responses. Results demonstrated that addition of filler material has a major influence on output response [22]. But, the optimal input parameters for achieving better outcome vary, depending on the response considered. Hence, it is essential to identify the common optimal parameter combination for all the responses considered.

Multi-objective optimization is a powerful tool for tackling a complex problem and prioritizes the problem at hand. Different materials and thicknesses require varying parameter settings. By optimizing parameters, the AWJM process can be adapted to cut a wide range of materials effectively, expanding its versatility and applications. Various

multi-objective optimization techniques, such as grey relational analysis (GRA), Technique for Order of Preference by Similarity to Ideal Solution (TOPSIS), principal component analysis (PCA), weighted aggregated sum product assessment (WASPAS) and Complex Proportional Assessment (COPRAS), are used by researchers to optimize the materials and process parameters to attain combined output responses [23, 24]. However, these techniques have some drawbacks such as assigning weights to criteria, sensitivity to the normalization, linearity in assumptions and interpretability challenges. Among the available methods, COPRAS has some unique advantages in terms of relative comparison of alternatives, and versatility across different types of data, making it a promising choice for optimizing machining parameters. Another problem in multi-objective optimization technique is assessment of weightage to output parameters [25]. This issue can be sorted by combining two optimization techniques in which weightage of output parameters can be calculated in one technique and the assigned weightage can be used in another technique to attain combined parameter setting for the output values. Criterion Importance Through InterCriteria Correlation (CRITIC) method has several advantages in the context of multi-criteria decision analysis. One of the primary advantages of CRITIC is its ability to consider the intercriteria correlation. By analysing how each criterion is related to every other criterion, CRITIC provides a more comprehensive understanding on the relationships and dependencies between different decision criteria. It calculates dynamic weights for each criterion based on their importance [26, 27].

Based on literature, it can be depicted that addition of filler materials increases the functional and mechanical properties of composites while affecting machinability. Implementation of optimization techniques is beneficial in advanced manufacturing processes where it is crucial to control material removal rate (MRR), surface roughness (Ra) and kerf taper (Kt). Increased machining capabilities could be beneficial for industries like automotive, aerospace and electronics. The optimized parameters could contribute to the manufacturing of high-strength and lightweight parts for various applications. To apply the composite in the manufacturing of electronic enclosures and components, both structural integrity and machining precision are essential. The filler addition's impact on reducing cracks, and craters could be particularly advantageous in electronic device manufacturing. Usage of mineral clays and nitride-based hybrid nanofillers for polymer composite development and its effect on machinability through AWJM have been rarely reported. Hence, an attempt has been made to study the machining characteristics of FRP composite developed with hybrid fillers consisting of MMT and boron nitride (BN). Herein, constant percentage of MMT and varying percentages of BN were selected as filler material. Taguchi method is used

for planning the experimental trails owing to its simplicity. A novel hybrid optimization approach, namely integrated Taguchi-COPRAS-CRITIC method, is used to perform multi-objective optimization of AWJM process to attain an optimal set of output response. CRITIC is used to calculate the weightage for each output, and the assigned weights are used in COPRAS to optimize the machining parameters.

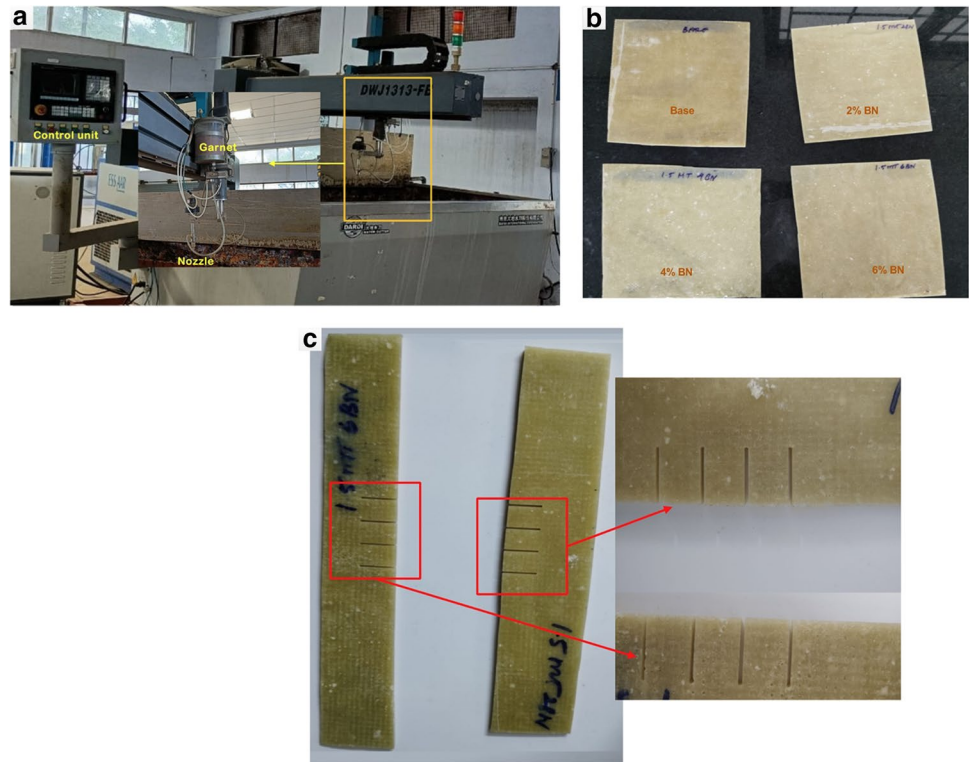
## 2 Materials and methods

Herein, HY951 grade hardener and LY 556 grade epoxy are selected as base matrix materials while keeping a 1:10 ratio. The chosen epoxy grade has an acceptable dimension stability that makes it a popular base matrix. The fundamental and practical qualities of the epoxy may be enhanced by adding a right amount of filler and reinforcing material. Glass fibres with 200 g per square meter (GSM) are chosen as the reinforcing fibre at 30 weight percentage (wt%) in epoxy matrix. Based on reviews of the literature, it was found that 30 wt% of glass fibre is the ideal amount to improve the mechanical properties of base matrix, and the addition of BN fillers up to 6 wt% displays improved mechanical and flame retardancy capabilities [27]. To improve the thermal behaviour and effectiveness in binding between base matrix materials with reinforcement, MMT nanoclay with 50–100 nm range in size and BN were utilized as filler materials. The weight percentage of MMT in this study was set at 1.5 wt%, while the weight percentage of boron nitride was changed at a constant range of 2 to 6 wt% (Fig. 1b).

## 3 Composite fabrication

The development of planned epoxy/glass fibre composite combinations is done through the compression moulding method. Firstly, the calculated weight percentage of filler material is ultrasonically treated individually with ethanol for 1 h. Later achieving the desired dispersion, the solution of filler is ultrasonically combined up to 2 h. After being introduced to the epoxy matrix, the dispersed hybrid filler is agitated mechanically for 2 h at a speed of 1200 rpm. The matrix filler mixture is then supplemented with HY951 hardener at a determined ratio of 1:10. The matrix filler mixture is first coated on glass fibre using the hand layup process. Coated glass fibre is stacked as plates for 30 mm thickness and degassed thereafter. A hot press is used to provide 15 MPa of pressure to the stacked polymer matrix, which is then subjected to a curing procedure [4]. The remaining set of composites are created using the same process but with varying filler additions as given in Section 2.

**Fig. 1** **a** Abrasive water jet machine setup. **b** Fabricated composite. **c** Composite specimen after machining



## 4 Machining parameters

Using an abrasive water jet machine, the produced composite's machinability is studied. Here, a DIPS6-2230 high-pressure pump and a DWJ1313-FB water jet cutter having an impact angle of  $90^\circ$  and 0.70-mm-diameter aperture are the main components of AWJM. Figure 1 shows the garnet sand abrasive particle in AWJM (80 mesh). SOD, TS and WP are chosen as the input parameters based on the literature review and expert console. For planning experiments and to comprehend the effects of selected parameters, the conventional Taguchi approach is used. In this study, the experimental strategy includes three components, each at three levels (Table 1). A Leica microscope and an image analyser are used to calculate the distance between machined slots as the output parameter, which is the kerf taper. For the sake of accuracy, three readings have been made from various locations of slots between machined surfaces, and the mean values have been calculated (Fig. 1c).

**Table 1** Levels and parameters

	Unit	Notation	Level 1	Level 2	Level 3	Level 4
Filler %	wt%	Filler %	0	2	4	6
Water pressure	MPa	WP	200	230	260	290
Transverse speed	mm/min	TS	30	40	50	60
Stand-off distance	mm	SOD	1	2	3	4

The L16 orthogonal array designed through Minitab 16 software is given in Table 2 along with the measured experimental outcome values. The obtained results, namely kerf taper, surface roughness and removal of material, are converted into signal-to-noise (SN) ratio by selecting suitable criteria with larger the better or smaller the better. The obtained SN ratio values are also provided in Table 2, which is used to build the main effect plots showing the effect of each parameter on response.

## 5 Results and discussion

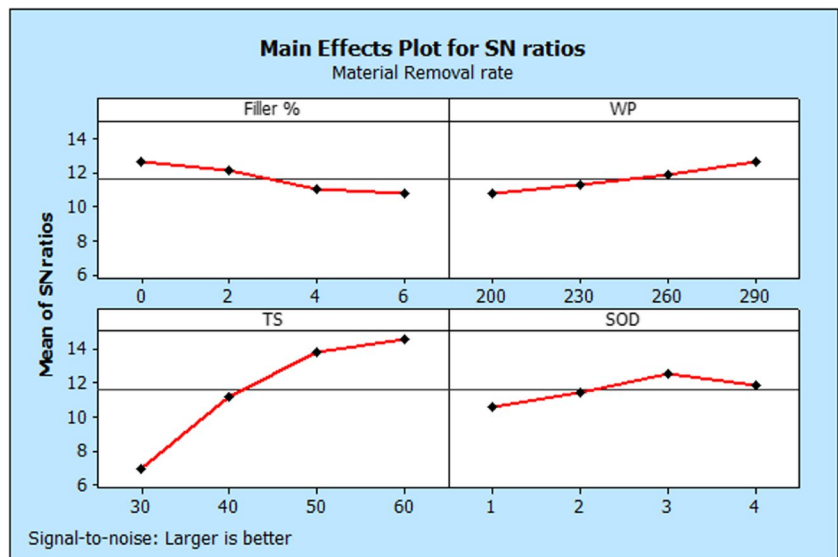
### 5.1 Effect of machining parameters on material removal rate

Influence of control factors over MRR is depicted in Fig. 2. It can be seen that increases in filler addition decreases MRR of developed composite. Herein, an increase in addition of filler material improves the bonding among the

**Table 2** Experimental results

Exp. no	Filler %	WP	TS	SOD	MRR	Ra	Kt	SN ratio for MRR	SN ratio for Ra	SN ratio for Kt
1	0	200	30	1	2.03	3.57	0.5336	6.1499	-11.0534	5.45568
2	0	230	40	2	4.05	3.59	0.5667	12.1491	-11.1019	4.93294
3	0	260	50	3	6.07	3.87	0.6959	15.6638	-11.7542	3.14906
4	0	290	60	4	6.75	3.99	0.7409	16.5861	-12.0195	2.60481
5	2	200	40	3	3.72	3.71	0.6144	11.4109	-11.3875	4.23098
6	2	230	30	4	2.25	3.55	0.6016	7.0437	-11.0046	4.41384
7	2	260	60	1	5.51	3.66	0.5519	14.8230	-11.2696	5.16279
8	2	290	50	2	5.64	3.63	0.5061	15.0256	-11.1981	5.91527
9	4	200	50	4	4.53	3.84	0.7244	13.1220	-11.6866	2.80043
10	4	230	60	3	5.31	3.86	0.6616	14.5019	-11.7317	3.58809
11	4	260	30	2	2.01	3.3	0.3919	6.0639	-10.3703	8.13649
12	4	290	40	1	3.27	3.24	0.4061	10.2910	-10.2109	7.82734
13	6	200	60	2	4.16	3.89	0.6016	12.3819	-11.7990	4.41384
14	6	230	50	1	3.65	3.57	0.4399	11.2459	-11.0534	7.13292
15	6	260	40	4	3.44	3.52	0.5072	10.7312	-10.9309	5.89642
16	6	290	30	3	2.72	3.23	0.3492	8.6914	-10.1841	9.13852

**Fig. 2** Main effects plot for material removal rate



fibre and base resin matrix with better interfacial adhesion. This fact makes the erosion or material removal rate of composite a difficult task. Increases in WP increase the MRR, and this might owe to the influence of kinetic energy. During machining condition upsurge in water jet pressure increases the kinetic energy of abrasive particles that strike over the work sample and erodes the materials in machining zone. It can also be observed that increases in transverse speed increases the MRR, these abrasive water jet particles erode the composite surface at a faster rate with respect to increment in transverse speed, thus increasing the MRR. Due to this fact, more deeper cracks are developed on work sample in chip formation which

leads to greater MRR. Likewise, intermolecular forces and energy generated in abrasive water jet particle have a major impact at higher transverse speed. Stand-off distance increment results in higher MRR due to the divergence in abrasive water jet [18]. Increases in SOD result in scattering of jet to cover more area in work sample, which leading to higher MRR. Table 3 summarizes the response for MRR, and it indicates that transverse speed acts as the most significant parameter in governing MRR, followed by stand-off distance, while filler wt% has a minimal effect on MRR.

The significance of control factors for MRR is summarized in Table 4, which shows results from analysis of

**Table 3** Response for MRR

Levels	Filler %	WP	TS	SOD
1	12.637	10.766	6.987	10.627
2	12.076	11.235	11.146	11.405
3	10.995	11.82	13.764	12.567
4	10.763	12.648	14.573	11.871
Delta	1.875	1.882	7.586	1.94
Rank	4	3	1	2

variance (ANOVA) with a  $P$  value less than 0.05. It can be seen that all the control factors have significance over the MRR. Furthermore, for each control factor, its individual contribution to output response can be calculated by dividing the total sequential sums of squares values with the individual sequential sums of squares values of each control factor. Herein, transverse speed has the major contribution of ~76.36% and filler weight percentage has the second major contribution (~11.01%) in governing the MRR values, followed by water pressure and stand-off distance. Both ANOVA and SN ratio analysis show that transverse speed is the most significant parameter. It should be noted that based on ANOVA, there is a slight variation in contribution on influencing parameters as it is concerned with explaining a variation in a dependent variable, while SN ratio analysis is focused on optimizing a process by maximizing the signal and minimizing noise.

Combined influence of input parameters on MRR is depicted in Fig. 3. Figure 3a shows the combinational effect of filler wt% and water pressure on MRR of the developed composite. It can be seen that MRR values are lower at minimal filler wt% and water pressure when WP < 240 MPa. At minimal WP, the kinetic energy of the abrasive particle is lower, resulting in poor MRR. Herein, MRR values are higher at minimal level of filler material and maximum level of water pressure. At 0 wt% filler condition, the strength of the base material is low and higher level of WP surges the kinetic energy of garnet particles that results in high MRR values. Effect of stand-off distance and transverse speed on MRR is depicted in Fig. 3b. Herein, MRR is at maximum at maximum level of control factor, higher stand-off

distance results in divergence in abrasive water jet flow and high transverse speed increases the constant hitting of water jet over work samples. At maximum transverse speed, the movement of water jet over composite surface will be higher, which results in continuous hitting of abrasive water jet over the machine zone, thus improving the MRR values. Influence of filler wt% and transverse speed on MRR is depicted in Fig. 3c. It can be seen that minimal transverse speed and filler wt% decrease the MRR, since a decrease in transverse speed reduces the chance of abrasive water jet particle hitting. Effect of stand-off distance and water pressure is depicted in Fig. 3d. It can be notified that MRR values are minimal at minimal levels of control factor, since lower stand-off distance results in formation of unstable jet [28]. This divergence decreases the concentration of abrasive particles that causes fluctuations in pressure and flow, thus decreases the MRR.

## 5.2 Effect of machining parameters on surface roughness

Influence of machining parameters on Ra is depicted in Fig. 4. It can be observed that Ra decreases with an increase of filler addition. This might be due to the increase of the interfacial bonding strength. The addition of filler material reduces the microvoids and results in smooth surface at the time of erosion caused by water jet particles. An increase in filler percentage decreases surface roughness since the filler materials will get eroded by abrasive water jet particles through brittle mechanism, thus forming smooth machined surface. However, the base matrix materials are abraded by tearing or ductile cutting mechanism which increases the roughness of the developed composites. Surface roughness of composite decreases with an increase in WP; herein, as WP increases, the kinetic energy of abrasive jet particles increases, thus improving the surface roughness. Lower WP results in jet deflection that causes greater waviness in machined surface. An increase in transverse speed decreases the quality of the machined surface due to the contribution of insufficient quantity of abrasive particles at machining condition. At lower transverse speed, the contribution of abrasive particle is higher, which results in

**Table 4** ANOVA for MRR

Source	df	Seq SS	Adj SS	Adj MS	F	P	Contribution (%)
Filler %	3	3.5629	3.5629	1.1876	23.6	0.014	11.01
WP	3	2.3496	2.3496	0.7832	15.56	0.025	7.26
TS	3	24.7069	24.7069	8.2356	163.66	0.001	76.36
SOD	3	1.5841	1.5841	0.528	10.49	0.042	4.90
Error	3	0.151	0.151	0.0503			
Total	15	32.3545					

$$R^2 = 99.53\%$$

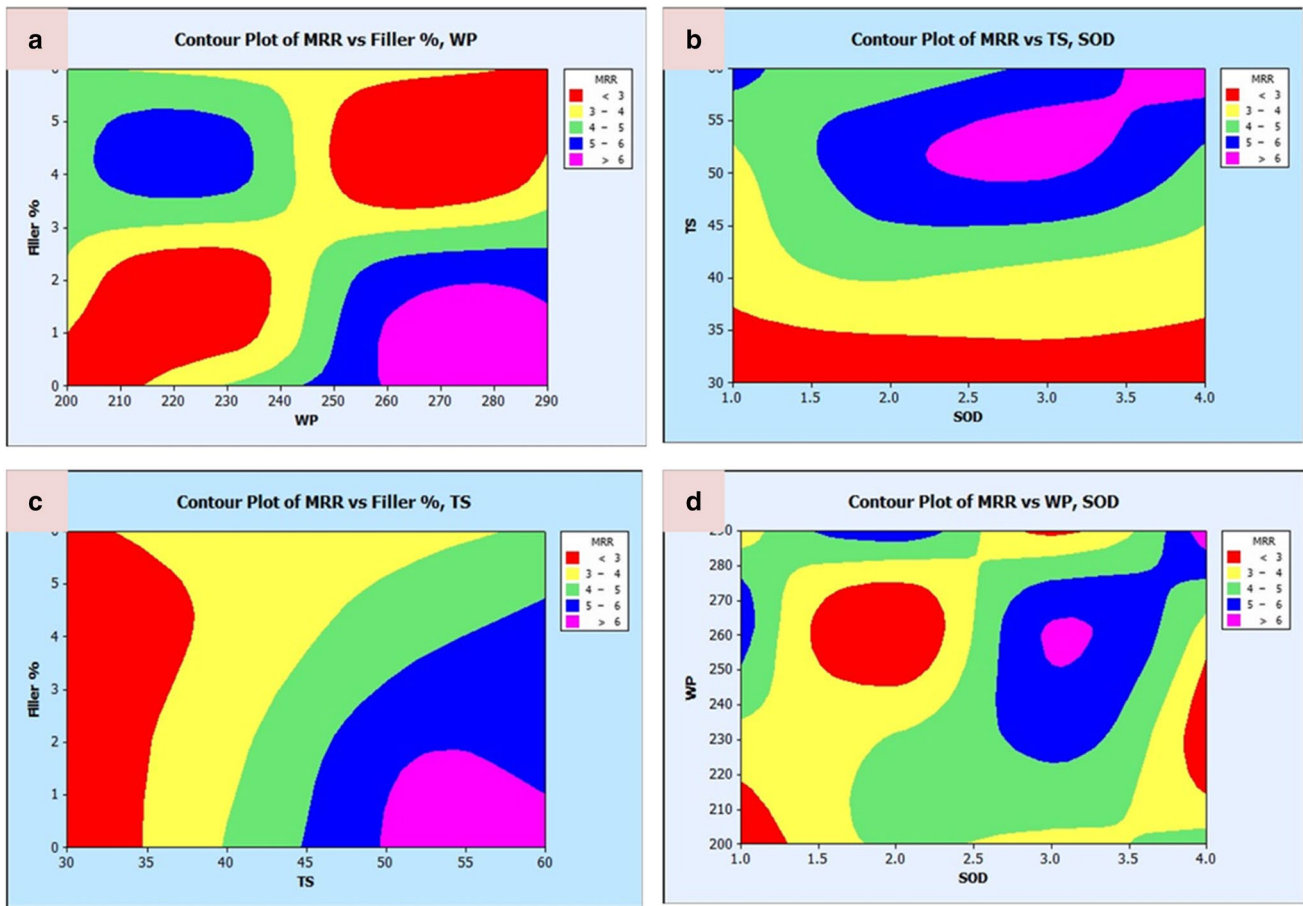
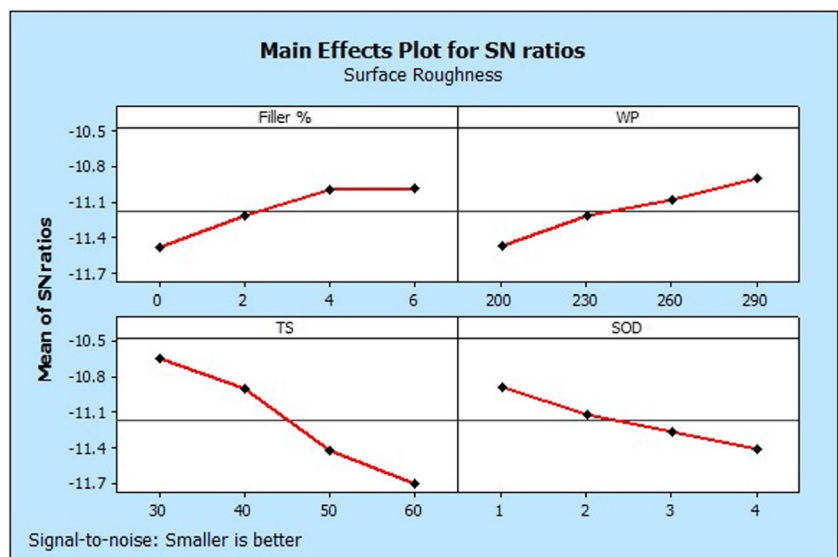


**Fig. 3** Contour plots showing the combined effect of input parameters on MRR. **a** Filler % and WP. **b** TS and SOD. **c** Filler % and TS. **d** WP and SOD

**Fig. 4** Main effects plot for surface roughness





suitable machining time for abrasive jet particle interaction over composites, leading to lower surface roughness. However, higher transverse speed causes flaws and permits less overlap action over machined surface, and also it reduces hitting of garnet particles on composite surface, resulting in an increase in the surface roughness value. Higher SOD values increase the surface roughness, and this might be due to the decreases in kinetic energy of garnet particles caused by the longer distance between the work sample and nozzle. This fact results in divergence of abrasive jet that forms jet in wider jet diameter and increases the interaction volume, thus decreasing the density of kinetic energy of the jet particles. As a result, the penetration capability of jet particles decreases, thus decreasing the quality of surface finish [29].

Table 5 summarizes the response for Ra, it can be seen that the transverse speed acts as the major significant factor on surface roughness, followed by water jet pressure, and filler wt% has the least effect on Ra. Significance and contribution of individual parameters on surface roughness can be obtained from ANOVA (Table 6). As depicted in Table 6, transverse speed has the major influence on governing the surface roughness of composite with a contribution percentage of 58.66%. Water jet pressure has 14.11% of contribution, and filler wt% has the contribution percentage of 13.15%.

Collective effect of control factor on Ra is depicted in Fig. 5. Figure 5a reveals that surface roughness values are lower at higher level of water pressure and filler wt%. During machining condition, higher water pressure increases the pressure of abrasive particles that erode the composite surface without any damages; likewise, an increase in fillers

increases the brittleness of the developed composite which results in smoother surface finish. Effect of transverse speed and stand-off distance on surface roughness is depicted in Fig. 5b. It can be notified that surface roughness was lower at minimal level of transverse speed and stand-off distance. During the above set condition, the distance between nozzle and composite was minimal which increases the penetration action of abrasive jet particle and results in improvement of the surface quality. Likewise, minimal transverse speed increases the chance of interaction between the work sample and jet particles, which allows constant hitting of jet at a particular surface of composite sample without any divergence, thus decreasing the surface roughness. Figure 5c depicts the influence of filler wt% and transverse speed on surface roughness values. Herein, maximum level of filler wt% and minimal level of transverse speed improve the smoothness of machined surface. This might be due to the improvement of bonding property among fibre and base matrix material, and this confirms the protection of machined surface from extreme erosion at the time of cutting process. Combined influence of water pressure and stand-off distance is depicted in Fig. 5d. Herein, higher level of water pressure and lower level in SOD deliver lower surface roughness. When the abrasive jet particles are transported with higher WP, the kinetic energy of abrasive jet particles increases which improves the proficiency of smother surface finish [30].

### 5.3 Effect of machining parameters on kerf taper

Figure 6 depicts the effect of machining parameters on kerf taper. It can be seen that higher filler % and water pressure decrease the kerf taper. For lower WP, the kinetic energy of garnet jet particles decreases which results in smaller depth of penetration. This increases the kerf angle that showcases negative influence in machining behaviour. Higher water pressure delivers consecutive momentum to abrasive water jet particle that forms a wider kerf taper at bottom, thus lowering the kerf taper. Another reason is that a decrease in water pressure creates pressure drops in jet particle that decrease its sharpness. Kerf taper is directly related with the time of interaction between work sample and abrasive jet particles. Herein, a decrease in transverse speed decreases

**Table 5** Response for Ra

Level	Filler %	WP	TS	SOD
1	- 11.48	- 11.48	- 10.65	- 10.9
2	- 11.21	- 11.22	- 10.91	- 11.12
3	- 11	- 11.08	- 11.42	- 11.26
4	- 10.99	- 10.9	- 11.7	- 11.41
Delta	0.49	0.58	1.05	0.51
Rank	4	2	1	3

**Table 6** ANOVA for Ra

Source	df	Seq SS	Adj SS	Adj MS	F	P	Contribution (%)
Filler %	3	0.106125	0.106125	0.035375	9.21	0.049	13.15
WP	3	0.113875	0.113875	0.037958	9.88	0.046	14.11
TS	3	0.473525	0.473525	0.157842	41.09	0.006	58.66
SOD	3	0.102125	0.102125	0.034042	8.86	0.053	12.65
Error	3	0.011525	0.011525	0.003842			
Total	15	0.807175					

$R^2 = 98.57\%$

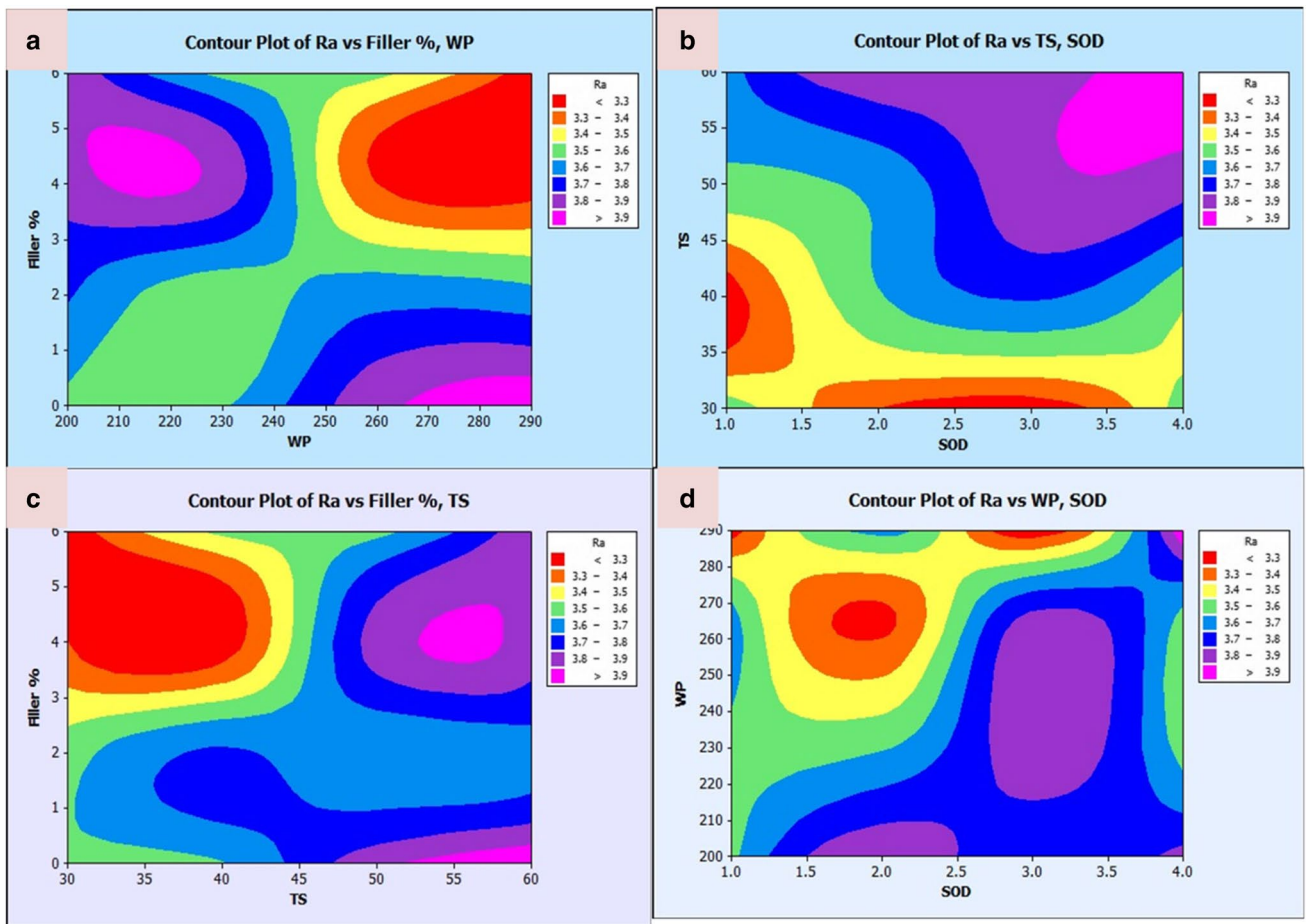
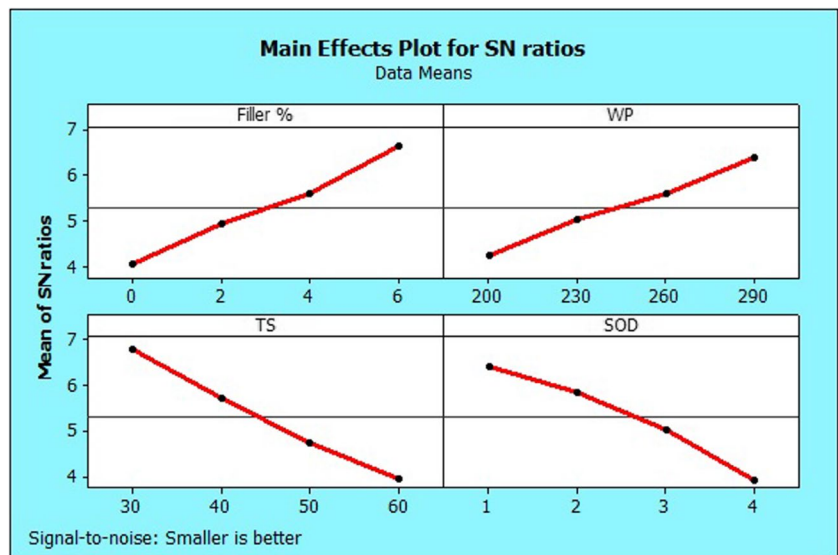


**Fig. 5** Contour plot showing the combined effect of input parameters on Ra. **a** Filler % and WP. **b** TS and SOD. **c** Filler % and TS. **d** WP and SOD

**Fig. 6** Main effects plot for kerf taper



the Kt, and this might be owing to the participation of minimal quantity of water jet particles, which reduces its penetration per unit area at higher transverse speed. An increase in filler wt% decreases the kerf angle, and this might be due to the better bonding strength that resists against the material erosion and thus decreases kerf taper. An increase in SOD increases the kerf taper, and it might be due to the higher energy disbursement over the composite specimen, which leads to non-uniform surface and difficulties in measuring the kerf taper. Table 7 depicts that transverse speed acts as the major significant parameter on governing the kerf taper, followed by filler wt%, and water pressure has the lowest inference on kerf taper of the developed composite. From ANOVA results (Table 8), it can be seen that all the parameters have effects on kerf taper since the values of *P* are less than 0.05. Herein, transverse speed has higher contribution of 31.63% followed by stand-off distance with 28.59% of contribution. Wt% of filler has the third contribution percentage of 24.59%, and water pressure has lower contribution of 14.12%.

Influence of control factors in a combined form is depicted in Fig. 7. Effect of filler wt% and water pressure is illustrated in Fig. 7a, and it can be seen that kerf taper values are lower at higher levels of filler addition and water pressure. This may be due to the dynamic performance of abrasive jet particles that concentrate more on the marked surface, which increases the energy fluctuation and decreases the chance of narrow kerf. From Fig. 7b, it can be observed that lower kerf taper was obtained at lower level of transverse speed and medium level of

stand-off distance. At the mentioned position, minimal transverse speed increases the interaction between the jets and machined surface, resulting in proper penetration of jet which decreases the kerf taper. The mechanism happens in the combined effect of filler wt% and transverse speed. Higher filler wt% improves the brittleness of composite which minimizes the chance of tearing of fibres and base matrix. Likewise, at higher water pressure and minimal stand-off distance, the kerf taper was minimal since lower stand-off distance decreases the divergence of jet and high water pressure increases the fine cutting of surface, thus decreasing kerf taper.

### 5.4 Multi-objective optimization by CRITIC-coupled COPRAS approach

#### 5.4.1 Development of CRITIC modelling

The purpose of multi-objective optimization is to find the parameter combinations that produce mutually optimum output for two or more variables. The main challenge in multiple response optimization is choosing an accurate weight for the output response. Based on experience with the use of the trial-and-error approach in relation to the relevance of the control factors, researchers have assessed the weightage for the response [25]. Therefore, a novel method of determining the weightage for the output response has to be developed. In this study, CRITIC is used to assign individual weights to output responses. In order to assign weights to their features and parallelize comparisons with real-world situations, decision makers frequently communicate their views by taking into consideration choice factors [31]. Since CRITIC weight measures a criterion’s importance based on how it ranks relative to others, this decision is not necessary when using the CRITIC technique. CRITIC provides a systematic and structured approach to decision-making, considering the interdependencies between criteria. It helps decision-makers avoid subjective biases and make more informed choices. The following stages were used to illustrate the CRITIC approach [26].

**Table 7** Response for Kt

Level	Filler %	WP	TS	SOD
1	4.036	4.225	6.786	6.395
2	4.931	5.017	5.722	5.85
3	5.588	5.586	4.749	5.027
4	6.645	6.371	3.942	3.929
Delta	2.61	2.146	2.844	2.466
Rank	2	4	1	3

**Table 8** ANOVA for Kt

Source	df	Seq SS	Adj SS	Adj MS	F	P	Contribution (%)
Filler %	3	0.052118	0.052118	0.017373	22.65	0.015	24.59
WP	3	0.029923	0.029923	0.009974	13	0.032	14.12
TS	3	0.067041	0.067041	0.022347	29.13	0.01	31.63
SOD	3	0.060605	0.060605	0.020202	26.34	0.012	28.59
Error	3	0.002301	0.002301	0.000767			
Total	15	0.211987					

$R^2 = 98.91\%$

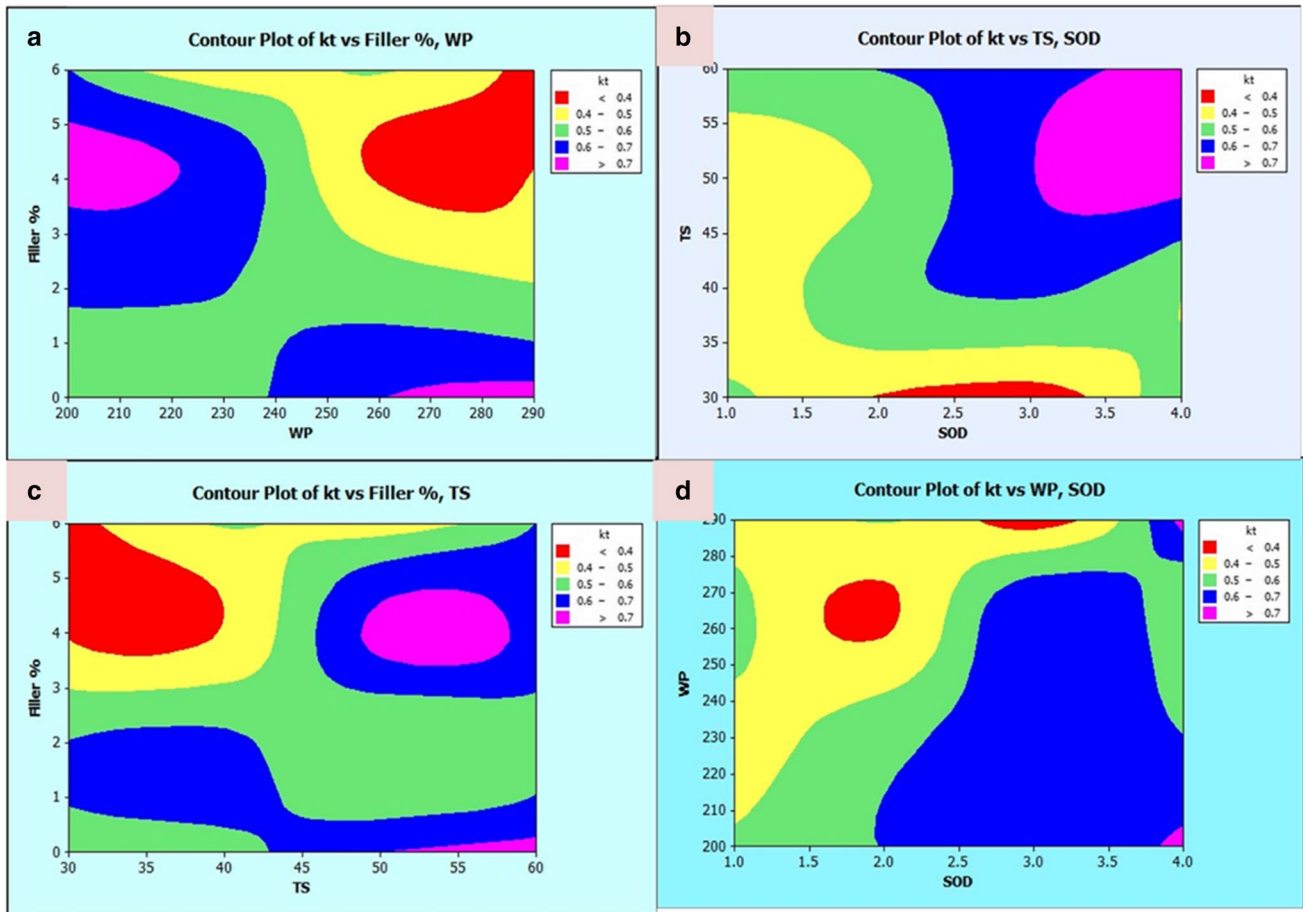


**Fig. 7** Contour plot showing the combined effect of input parameters on Kt. **a** Filler % and WP. **b** TS and SOD. **c** Filler % and TS. **d** WP and SOD

*Step 1:* Construction of decision matrix based on output values shown in Eq. (1)

$$D = [D_{ij}]_{n \times m} = \begin{bmatrix} D_{11} & D_{12} & \dots & D_{1m} \\ D_{21} & D_{22} & \dots & D_{2m} \\ \dots & \dots & \dots & \dots \\ D_{n1} & D_{n2} & \dots & D_{nm} \end{bmatrix} \quad (1)$$

where  $D_{ij}$  is the performance data of the  $j$ th response of  $i$ th design.

*Step 2:* Normalization of attained decision matrix using Eq. (2) where  $\min(D_{ij})$  denotes the minimal function and  $\max(D_{ij})$  represents the maximum function. The normalized values are showcased in Table 9. Herein, for MRR, the higher value is selected as maximum function, while lower values are selected as maximum function for surface roughness and kerf angle.

$$D_{ij}^+ = \frac{D_{ij} - \min(D_{ij})}{\max(D_{ij}) - \min(D_{ij})} \quad (2)$$

**Table 9** Normalized decision matrix obtained in the CRITIC method

Run	Normalization MRR	Normalization Ra	Normalization Kt
1	0.0042	0.5526	0.5292
2	0.4304	0.5263	0.4447
3	0.8565	0.1579	0.1149
4	1.0000	0.0000	0.0000
5	0.3608	0.3684	0.3230
6	0.0506	0.5789	0.3556
7	0.7384	0.4342	0.4825
8	0.7658	0.4737	0.5994
9	0.5316	0.1974	0.0421
10	0.6962	0.1711	0.2025
11	0.0000	0.9079	0.8910
12	0.2658	0.9868	0.8547
13	0.4536	0.1316	0.3556
14	0.3460	0.5526	0.7684
15	0.3017	0.6184	0.5966
16	0.1498	1.0000	1.0000

Step 3: Formulating the correlation coefficient by Eq. (3) where  $\sigma_j$  represents the standard deviation of  $j$ th response and  $r_{ij}$  represents the correlation coefficient among the output factors.

$$Co_j = \sigma_j \times \sum_{j=1}^n (1 - r_{ij}) \tag{3}$$

Step 4: Weight determination for each output response by using Eq. (4)

$$IW_j = \frac{Co_j}{\sum_{j=1}^n Co_j} \tag{4}$$

The calculated  $IW_j$  value from Eq. (4) is used in weightage calculation in COPRAS approach. Herein, the correlation coefficient and weightages are depicted in Table 10.

### 5.4.2 CRITIC-coupled COPRAS approach

The COPRAS technique includes direct confidence and proportion in importance and efficacy in substitutes that are possible when there are equally conflicting parameters [32]. COPRAS associates the weights based on the ranking and

**Table 10** Correlation and individual weightage

	MRR	Ra	Kt	$Co_j$	$IW_j$
MRR	1	-0.7358	-0.6347	1.0443	0.4930
Ra	-0.7358	1	0.9214	0.5538	0.2615
Kt	-0.6347	0.9214	1	0.5200	0.2455

**Table 11** Computed attribute values

Normalized matrix			Weighted normalized matrix			$P_i$	$R_i$
MRR	Ra	Kt	MRR	Ra	Kt	MRR	Ra
0.03110	0.06150	0.06000	0.02172	0.00138	0.01685	0.02172	0.01877
0.06220	0.06180	0.06372	0.04334	0.00139	0.01789	0.04334	0.01982
0.09320	0.06670	0.07825	0.06496	0.00149	0.02197	0.06496	0.02405
0.10360	0.06870	0.08331	0.07224	0.00154	0.02340	0.07224	0.02554
0.05710	0.06390	0.06909	0.03981	0.00143	0.01940	0.03981	0.02139
0.03450	0.06110	0.06765	0.02408	0.00137	0.01900	0.02408	0.02090
0.08460	0.06300	0.06206	0.05897	0.00141	0.01743	0.05897	0.01939
0.08660	0.06250	0.05691	0.06036	0.00140	0.01598	0.06036	0.01793
0.06950	0.06610	0.08146	0.04848	0.00148	0.02287	0.04848	0.02494
0.08150	0.06650	0.07440	0.05683	0.00149	0.02089	0.05683	0.02296
0.03080	0.05680	0.04407	0.02151	0.00127	0.01238	0.02151	0.01415
0.05020	0.05580	0.04567	0.03499	0.00125	0.01282	0.03499	0.01456
0.06380	0.06700	0.06765	0.04452	0.00150	0.01900	0.04452	0.02109
0.05600	0.06150	0.04947	0.03906	0.00138	0.01389	0.03906	0.01581
0.05280	0.06060	0.05703	0.03681	0.00136	0.01602	0.03681	0.01791
0.04170	0.05560	0.03927	0.02911	0.00125	0.01103	0.02911	0.01276

recommends better ideal control factors, using success of alternatives in connection to numerous control aspects. The following steps are involved in the COPRAS approach [33].

Step 1: The initial step the choice matrix is created, then the output parameter is normalized by

$$NO_{ij} = \frac{Q_{ij}}{\sqrt{\sum_{i=1}^m Q_{ij}^2}} \tag{5}$$

where  $NO_{ij}$  is the normalized matrix,  $Q_{ij}$  is the value in the choice matrix and  $m$  is the number of alternatives.

Step 2: Calculated individual weight is multiplied to a normalized decision matrix in this process as shown in Eq. (6). Here, the normalized matrix (Eq. (5)) will be multiplied by the weightage computed from the CRITIC approach (Eq. (4)) to create the weighted matrix displayed in Table 11 where  $NW_{ij}$  is the weighted normalized value.

$$NW_{ij} = IW_j \times NO_{ij} \tag{6}$$

Step 3:  $P_i$  calculation where  $P_i$  denotes the maximization of function calculated using Eq. (7) and  $n$  is the number of maximum response. In this research, MRR is considered as the maximization since higher MRR improves the machining performance.

$$P_i = \sum_{j=1}^n Q_{ij} \tag{7}$$

Step 4: Calculation of  $R_i$  where  $R_i$  implies the minimization of the function calculated based on Eq. (8). Herein,

Ra and Kt are considered as the minimization function since lower Ra and Kt deliver better surface quality.

$$R_i = \sum_{j=m+1}^n Q_{ij} \tag{8}$$

Finally, the summarized calculated data are shown in Table 11.

Step 5: Perceiving the diminutive value of R

$$R_{\min} = \min R_i \tag{9}$$

Step 6: Weight determination on individual response  $Q_i$

The  $Q_i$  values are calculated by using Eq. (10), and the highest value in  $Q_i$  is denoted as  $Q_{\max}$ .

$$Q_i = P_i + \frac{R_{\min} \sum_{j=1}^m R_i}{R_i \sum_{j=1}^m R_{\min} / R_i} \tag{10}$$

Step 7: Utility degree  $N_i$  % determination

$$N_i = 100 \times (Q_i / Q_{\max}) \tag{11}$$

Based on the maximum value of utility degree, optimal parameters are ranked and respective values are depicted in Table 12.

It is possible to obtain better MRR using the CRITIC-coupled COPRAS method as well as minimal Ra and kerf taper by using the optimal control factors. To achieve better production rate with high quality in machined surface,

lower pulse off time and filler combined with higher values of pulse on time and wire feed rate are optimal control factors for machining the developed composite. In the hybrid approach, the optimal cutting parameters obtained (highlighted in italicized font in Table 12) are 290 MPa water pressure, 60 mm/min transverse speed and 4 mm SOD which yield 16.20 mm<sup>3</sup>/min of MRR with 0.29° kerf taper angle and 3.86 μm minimal surface roughness.

### 5.5 Surface morphology of machined surface

The optimal machining parameters suggested by CRITIC-coupled COPRAS are adopted to machine the developed composite with various filler percentages. Machined surface at optimal setting on the developed composite is depicted in Fig. 8a–d. Formation of cracks and larger craters were identified for composite made without filler addition (Fig. 8a), and this might be due to poor bonding among the fibres and base resin matrix. We can also observe some pull-out of fibres which might be due to the relatively high water pressure, which improves the impact energy of water jet particles [17]. This poorly bonded composite has minimal strength to withstand the impacted pressure, which results in tearing or debonding of fibres from the base matrix. Occurrence of ductile mechanism has been identified for composite with addition of fillers (Fig. 8b–d). The reason might be due to lower interaction, and the filler materials will have the capacity to withstand the pressure, after which the fibre starts to be cut down and form a smoother surface. Likewise, cavities are formed due to the matrix fall-out and missing fibre segment. Abrasive particles were observed over the machined surface with interlaminar delamination. Herein, for the tensile failure, adiabatic shear zones are the major mechanisms in material failure. The interaction of the water jet at high speed with the surface frequently results in delamination [34]. A significant component that can alter the mechanical behaviour of composite systems during processing such as water jet cutting is delamination. The findings of the experiment suggest that the lack of abrasive grains during water jet cutting might potentially contribute to delamination. At the optimal cutting condition of WP = 290 MPa, TS = 60 mm/min and SOD = 4 mm, for composite with a higher filler addition voids, the creation of gaps between the fibre and matrix was observed, and this might be due to high cutting energy which initiates the fibre breakdown and causes the fibre withdrawal.

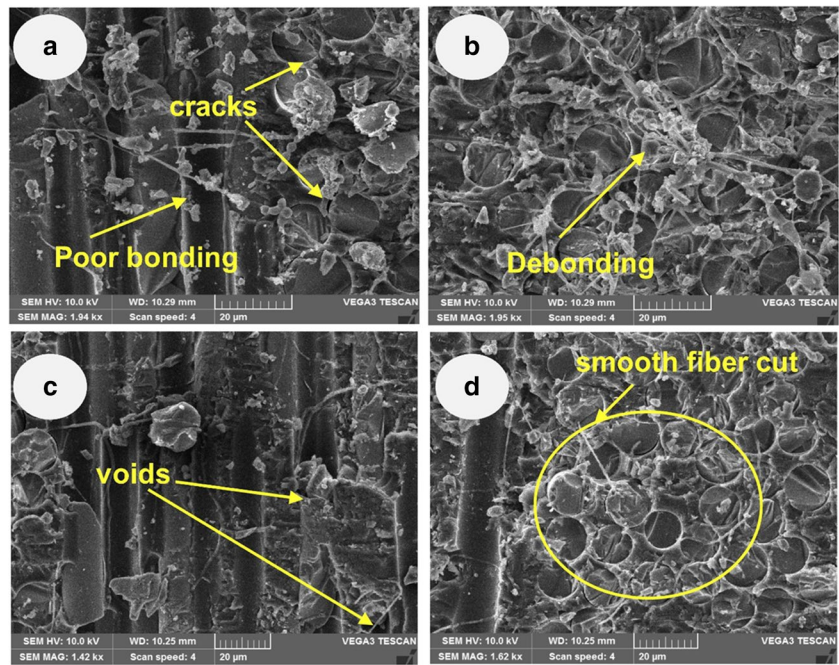
### 6 Conclusions

A novel glass fibre–reinforced epoxy composite filled with BN and MMT hybrid nanofillers is developed through compression moulding. Machinability of the developed

**Table 12** Optimality criterion and ranking

$R_{\min}/R_i$	$Q_i$	$N_i$ (%)	Ranking
0.67995	0.02226	30.50782	15
0.64373	0.04391	60.17605	8
0.53051	0.06565	89.96846	2
<i>0.49966</i>	<i>0.07297</i>	<i>100.00000</i>	<i>1</i>
0.59646	0.04042	55.39746	9
0.61045	0.02468	33.81810	14
0.65799	0.05952	81.57275	4
0.71166	0.06087	83.42221	3
0.51171	0.04919	67.41619	6
0.55566	0.05748	78.77912	5
0.90197	0.02191	30.03374	16
0.87620	0.03541	48.53018	12
0.60516	0.04512	61.83881	7
0.80722	0.03951	54.15225	10
0.71262	0.03732	51.15432	11
0.99994	0.02947	40.39294	13

**Fig. 8** Machined surface of **a** 0 wt% filler with WP=290 MPa, TS=60 mm/min and SOD=4 mm; **b** 2 wt% filler with WP=290 MPa, TS=60 mm/min and SOD=4 mm; **c** 4 wt% filler with WP=290 MPa, TS=60 mm/min and SOD=4 mm; and **d** 6 wt% filler with WP=290 MPa, TS=60 mm/min and SOD=4 mm



material is evaluated through AWJM. Implementing the optimization techniques is valuable in advanced manufacturing processes where precise control of MRR, Ra, and Kt is crucial. Industries such as aerospace, automotive and electronics could benefit from improved machining capabilities. The optimized parameters could contribute to the production of lightweight and high-strength parts for various applications. But, the research work on optimization of polymer composite machining is minimal and that too only few researchers considered filler quantity as input parameters. Hence, the current research aims to optimize the machining parameters along with filler quality for the developed novel composite. Taguchi method is used for experimental design, and CRITIC-weighted COPRAS method is adopted for attaining the optimal solution on higher MRR with minimal Ra and Kt. The following major conclusions can be drawn:

- Among all the input parameters, BN addition mainly affects the kerf taper, while stand-off distance and water pressure mainly affect the material removal rate and surface roughness. Increasing the addition of BN reduces the kerf taper and improves the surface finishing, although it also slightly reduces the material removal rate.
- ANOVA results depict that transverse speed is the most influencing parameter over all the considered responses with the highest average contribution of 55.55%, while water pressure has the lowest average contribution of 11.83%. Contour plot analysis reveals that combination of higher water pressure with minimal filler percentage delivers better MRR; however, the same condition

showcases higher values of surface roughness and kerf taper angle.

- CRITIC-COPRAS approach is able to identify the optimal cutting parameters (290 MPa water pressure, 60 mm/min transverse speed and 4 mm stand-off distance) for better production rate and high machined surface quality, leading to  $6.20 \text{ mm}^3/\text{min}$  of MRR with  $0.29^\circ$  kerf taper angle and  $3.86 \mu\text{m}$  minimal surface roughness.
- Formation of larger cracks and craters are identified on the machined surface through SEM analysis for the composite without filler addition, whereas a smooth machined surface is visualized for filler-added composites.
- In the future, machine learning approaches such as artificial neural network (ANN) and support vector machine (SVM) can be utilized to predict the MRR, Ra, and Kt for the developed novel composite by training the neural network with more experimental data.

**Author contribution** V. Kavimani: methodology, investigation, data curation, visualization and writing (first draft of the manuscript). P.M. Gopal: investigation. K.R. Sumesh: investigation. V. Sivamaran: investigation. W. Zhou: conceptualization, methodology, investigation, supervision and writing (reviewing and editing).

**Funding** Open access funding is provided by the University of Dundee.

**Data availability** The datasets used or analysed during the current study are available from the corresponding author on reasonable request.

**Code availability** Not applicable.

## Declarations

**Ethics approval and consent to participate** Not applicable.

**Consent for publication** Yes.

**Competing interests** The authors declare no competing interests.

**Open Access** This article is licensed under a Creative Commons Attribution 4.0 International License, which permits use, sharing, adaptation, distribution and reproduction in any medium or format, as long as you give appropriate credit to the original author(s) and the source, provide a link to the Creative Commons licence, and indicate if changes were made. The images or other third party material in this article are included in the article's Creative Commons licence, unless indicated otherwise in a credit line to the material. If material is not included in the article's Creative Commons licence and your intended use is not permitted by statutory regulation or exceeds the permitted use, you will need to obtain permission directly from the copyright holder. To view a copy of this licence, visit <http://creativecommons.org/licenses/by/4.0/>.

## References

- Balasubramani V, Boopathy SR, Stalin B, Kavimani V (2022) An experimental investigation on impact dynamics response of woven roved glass fiber reinforced polyester laminated composites. *Polym Compos* 43:7266–7277
- Kavimani V, Gopal PM, Sumesh KR, Elanchezian R (2022) Improvement on mechanical and flame retardancy behaviour of bio-exfoliated graphene-filled epoxy/glass fibre composites using compression moulding approach. *Polym Bull* 79:6289–6307
- Sumesh KR, Kavimani V, Rajeshkumar G, Ravikumar P, Indran S (2020) An investigation into the mechanical and wear characteristics of hybrid composites: influence of different types and content of biodegradable reinforcements. *J Nat Fibers* 19:2823–2835
- Cao Z, Li S, Li C, Li P, Ko TJ (2022) Formation mechanism and detection and evaluation methods as well as repair technology of crack damage in fiber-reinforced composite wind turbine blade: a review. *Int J Adv Manuf Technol* 120:5649–5672
- El Etri H, Korkmaz ME, Gupta MK, Gunay M, Xu J (2022) A state-of-the-art review on mechanical characteristics of different fiber metal laminates for aerospace and structural applications. *Int J Adv Manuf Technol* 123:2965–2991
- Madarvoni S, Rama SPS (2022) Dynamic mechanical behaviour of graphene, hexagonal boron nitride reinforced carbon-kevlar, hybrid fabric-based epoxy nanocomposites. *Polym Polym Compos* 30:09673911221107289
- Li X, Wang J, Tian Y, Jiang X, Zhang X (2022) Thermal enhancement by constructing ordered-orienting hybrid network with modified boron nitride, graphene and carbon nanotubes in epoxy composite coatings. *Prog Org Coatings* 172:107078
- Hu D, Liu H, Guo Y, Yang M, Ma W (2022) Interfacial design of nanocellulose/boron nitride nanosheets composites via calcium ion cross-linking for enhanced thermal conductivity and mechanical robustness. *Compos Part A Appl Sci Manuf* 158:106970
- Rajasekaran T, Palanikumar K, Latha B (2022) Investigation and analysis of surface roughness in machining carbon fiber reinforced polymer composites using artificial intelligence techniques. *Carbon Lett* 32:615–627
- Alarifi IM (2023) A review on factors affecting machinability and properties of fiber-reinforced polymer composites. *J Nat Fibers* 20:2154304
- Vigneshwaran S, Uthayakumar M, Arumugaprabu V (2018) Abrasive water jet machining of fiber-reinforced composite materials. *J Reinf Plast Compos* 37:230–237
- Shi H, Giasin K, Barouni A, Zhang Z (2024) An experimental assessment and optimisation of hole quality in Al2024-T3 aluminium alloy during abrasive water jet machining. *Int J Adv Manuf Technol*. <https://doi.org/10.1007/s00170-024-13009-9>
- Mitchell B, Sadek A, Kinsey B (2022) Advantages of water drop-let machining over abrasive waterjet cutting of carbon fiber reinforced polymer. *Manuf Lett* 33:342–348
- Gopal PM, Kavimani V, Arunkumar K (2023) Multi-objective optimization on abrasive water jet machining of epoxy/glass fiber/grinding wheel particle composite through hybrid optimization technique. *Multiscale Multidiscip Model Exp Des* 6:697–707
- Sreekumar M, Purushothaman S, Srinivas MS, Katiyar JK, Sankar MR (2022) A review of additives in abrasive water jet machining and their performance. *Proc Inst Mech Eng J J Eng Tribol* 237:964–978
- Boopathi S, Thillaivanan A, Azeem MA, Shanmugam P, Pramod VR (2022) Experimental investigation on abrasive water jet machining of neem wood plastic composite. *Funct Compos Struct* 4:25001
- Dahiya AK, Bhuyan BK, Kumar S (2023) Abrasive water jet machining of glass fibre reinforced polymer composite: experimental investigation, modelling and optimization. *Int J Interact Des Manuf* 17:1933–1947
- Anand G, Perumal SV, Yuvaraj N, Palanikumar K (2021) Influence of abrasive water jet machining parameters on hybrid polymer composite. *J Inst Eng Ser C* 102:713–722
- Chenrayan V, Manivannan C, Shahapurkar K, Zewdu GA, Maniselvam N, Alarifi IM, Alblalaid K, Tirth V, Algahtani A (2022) An experimental and empirical assessment of machining damage of hybrid glass-carbon FRP composite during abrasive water jet machining. *J Mater Res Technol* 19:1148–1161
- Iyer NP, Arunkumar N (2022) Investigation of abrasive water jet machining parameters of bismaleimide composites. *Mater Manuf Process* 14:1642–1651
- Juvvala SR, Chebattina KR, Venkata Ramana VSN, Bommana D, Pathem UC (2022) Machinability aspects of nano MMT deposited GFRP composites to minimize the drilling induced delaminations. *J Inst Eng Ser C* 103:1169–1175
- Thakur RK, Singh KK (2020) Experimental investigation and optimization of abrasive water jet machining parameter on multi-walled carbon nanotube doped epoxy/carbon laminate. *Measurement* 164:108093
- Kalita K, Chakraborty S, Ghadai RK, Chakraborty S (2023) Parametric optimization of non-traditional machining processes using multi-criteria decision making techniques: literature review and future directions. *Multiscale Multidiscip Model Exp Des* 6:1–40
- Kavimani V, Paramasivam B, Sasikumar R, Venkatesh S (2023) A CRITIC integrated WASPAS approach for selection of natural and synthetic fibers embedded hybrid polymer composite configuration. *Multiscale Multidiscip Model Exp Des*. <https://doi.org/10.1007/s41939-023-00301-6>
- da M. Passos Neto G, Alencar LH, Valdes-Vasquez R (2023) Multiple-criteria methods for assessing social sustainability in the built environment: a systematic review. *Sustainability* 15:16231
- Silva NF, dos Santos M, Gomes CFS, de Andrade LP (2023) An integrated CRITIC and grey relational analysis approach for investment portfolio selection. *Decis Anal J* 8:100285
- Chakraborty S, Datta HN, Kalita K, Chakraborty S (2023) A narrative review of multi-objective optimization on the basis of ratio



- analysis (MOORA) method in decision making. *OPSEARCH* 60:1844–1887
28. Akıncioğlu S (2021) Investigation of effect of abrasive water jet (AWJ) machining parameters on aramid fiber-reinforced polymer (AFRP) composite materials. *Aircr Eng Aerosp Technol* 93:615–628
  29. Gopal PM, Kavimani V, Arunkumar K (2023) Multi-objective optimization on abrasive water jet machining of epoxy/glass fiber/grinding wheel particle composite through hybrid optimization technique. *Multiscale Multidiscip Model Exp Des* 6:697–707. <https://doi.org/10.1007/s41939-023-00177-6>
  30. Sreekumar M, Purushothaman S, Srinivas MS, Katiyar JK, Sankar MR (2023) A review of additives in abrasive water jet machining and their performance. *Proc Inst Mech Eng J J Eng Tribol* 237:964–978
  31. Kumar MS, Farooq MU, Ross NS, Yang C-H, Kavimani V, Adediran AA (2023) Achieving effective interlayer bonding of PLA parts during the material extrusion process with enhanced mechanical properties. *Sci Rep* 13:6800
  32. Krishankumar R, Garg H, Arun K, Saha A, Ravichandran KS, Kar S (2021) An integrated decision-making COPRAS approach to probabilistic hesitant fuzzy set information. *Complex Intell Syst* 7:2281–2298
  33. Mishra AR, Liu P, Rani P (2022) COPRAS method based on interval-valued hesitant Fermatean fuzzy sets and its application in selecting desalination technology. *Appl Soft Comput* 119:108570
  34. Demiral M, Abbassi F, Saracyakupoglu T, Habibi M (2022) Damage analysis of a CFRP cross-ply laminate subjected to abrasive water jet cutting. *Alexandria Eng J* 61:7669–7684. <https://doi.org/10.1016/j.aej.2022.01.018>

**Publisher's Note** Springer Nature remains neutral with regard to jurisdictional claims in published maps and institutional affiliations.